Heterogeneous Freezing of Aqueous Particles Induced by Crystallized $(NH_4)_2SO_4$, Ice, and Letovicite

Bilal Zuberi, Allan K. Bertram, Thomas Koop,† Luisa T. Molina, and Mario J. Molina*

Departments of Earth, Atmospheric and Planetary Sciences and of Chemistry, Massachusetts Institute of Technology, Cambridge, Massachusetts 02139

Received: January 7, 2001; In Final Form: April 27, 2001

Heterogeneous freezing of aqueous particles with solid inclusions of crystallized $(NH_4)_2SO_4$, ice, and letovicite were studied using optical microscopy and differential scanning calorimetry. For $(NH_4)_2SO_4-H_2O$ particles, the heterogeneous freezing temperature was found to be dependent on the morphology of the $(NH_4)_2SO_4$ solid. If the crystallized solid was in the form of microcrystals, the heterogeneous ice-freezing temperature was close to the eutectic temperature and the critical saturation with respect to ice was close to 1. However, if the solid was in the form of one or two large crystals, the heterogeneous freezing temperature was close to the homogeneous freezing temperature. For particles with one or two large $(NH_4)_2SO_4$ crystals in equilibrium with $(NH_4)_2SO_4-H_2O$ solution, we have estimated an upper limit of 1.5×10^{-5} s^{-1} μm^{-2} for J_{het} (heterogeneous nucleation rate of ice, immersion freezing mode). Our results for $NH_4HSO_4-H_2O$ particles show that when one or two large crystals of either ice or letovicite are present in the solution, the freezing temperature does not deviate significantly from the homogeneous freezing temperature, consistent with the $(NH_4)_2SO_4-H_2O$ experiments. Our work shows that the surface area and surface microstructure of crystalline solids present in aqueous aerosols can significantly change the heterogeneous freezing temperature and critical ice saturations and that heterogeneous ice nucleation induced by crystalline salts may be very important in the formation of upper tropospheric clouds.

1. Introduction

Upper tropospheric (UT) clouds play an important role in the Earth's climate by scattering and absorbing solar radiation and radiation given off by the Earth's surface.[1−4] In addition, these clouds play an important role in the chemistry of the upper troposphere. For example, recent field and laboratory work has shown that UT clouds can perturb chlorine chemistry and contribute to ozone depletion.[5−8]

UT clouds form when tropospheric aerosols cool in rising air parcels, take up water, and eventually freeze.[4,9,10] The freezing of ice in these aerosols can occur by either homogeneous or heterogeneous nucleation; the latter occurs on a solid substrate, such as dust. Since the presence of a solid substrate often reduces the free energy barrier for nucleation,[4,11] heterogeneous nucleation usually occurs at lower saturation ratios than homogeneous nucleation, that is, at warmer temperatures or lower relative humidities.

Until recently, homogeneous freezing of aqueous particles was considered to be the dominant formation mechanism of UT ice clouds.[9,12,13] Consequently, homogeneous freezing of aqueous particles has been investigated extensively.[9,12−20] Specifically, the freezing properties of binary and ternary solutions of $(NH_4)_2SO_4$, H_2SO_4, and H_2O have been investigated (on the basis of modeling results and field data, atmospheric particles are believed to contain these compounds).[21−23]

The homogeneous freezing temperatures of $H_2SO_4-H_2O$, $(NH_4)_2SO_4-H_2O$, and $NH_4HSO_4-H_2O$ particles have been determined in our laboratory using differential scanning calorimetry (DSC) and optical microscopy.[14,15,17] The experimental data show that large ice saturation ratios (S_{ice}) are needed for homogeneous nucleation. Such large saturations have been observed in the upper troposphere,[24−26] indicating that homogeneous nucleation is the formation mechanism of some upper tropospheric ice clouds. However, Heymsfield and Milosevich[27] and Heymsfield et al.[24] have reported that much lower ice saturations are required for formation of some continental UT ice clouds. These field measurements suggest that heterogeneous nucleation, in addition to homogeneous nucleation, is occurring in the upper troposphere.

Some liquid $(NH_4)_2SO_4-H_2SO_4-H_2O$ particles in the upper troposphere may contain a solid core of cystallized salt.[28,29] For example, Tabazadeh and Toon[28] have demonstrated using an equilibrium thermodynamic model[30] and laboratory efflorescence data[31] that liquid $(NH_4)_2SO_4-H_2SO_4-H_2O$ particles in the upper troposphere may contain solid ammonium sulfate or letovicite. The presence of these crystallized salts in UT aerosol particles may significantly reduce the temperatures and saturations required for ice formation, by providing sites for heterogeneous nucleation, and thus, changing the mode of formation of UT ice clouds from homogeneous nucleation to heterogeneous nucleation.

In this paper, we investigate the possibility that ice nucleation via the immersion freezing mode may occur on $(NH_4)_2SO_4$ crystals. We prepared droplets containing a solid $(NH_4)_2SO_4$ crystalline core enclosed by a liquid $(NH_4)_2SO_4-H_2O$ solution and determined the freezing temperatures of these droplets. In addition, we report conditions required for the immersion freezing of liquid $NH_4HSO_4-H_2O$ particles with solid inclusions of letovicite and ice.

* To whom correspondence should be addressed. Tel: (617) 253-5081. Fax: (617) 258-6525. E-mail: mmolina@mit.edu.
† Swiss Federal Institute of Technology, Zurich, Switzerland.

10.1021/jp010094e CCC: $20.00
Published on Web 06/07/2001

2. Experimental Technique

2.1. Optical Microscope. An optical microscope (Zeiss Axioskop 20) was used to investigate heterogeneous freezing. This technique has been previously employed in our laboratory to study the homogeneous freezing of ice in binary $H_2SO_4-H_2O$, $(NH_4)_2SO_4-H_2O$, and $NH_4HSO_4-H_2O$ particles.[14,15,17] Details of the technique and apparatus are described elsewhere.[14] Briefly, an optical microscope was equipped with a cold stage (Linkam BCS 196) that housed a quartz microcell. The bottom surface of the cell was pretreated with an organosilane (AquaSil, Hampton Research Inc.) to produce a monomolecular hydrophobic surface layer that minimized heterogeneous effects from the glass surface. Previous studies in our laboratory[14,15] have shown that this hydrophobic surface does not promote nucleation of ice. Particles, with sizes ranging from 10 to 55 μm, were deposited onto the hydrophobic surface with a nebulizer (Meinhard, TR30) and their concentrations were adjusted by exposing them to a fixed relative humidity. After adjusting the particle composition, Halocarbon grease (Halocarbon Products, Series 28LT) was added to the cell and the cell was sealed. This resulted in the aqueous particles forming an emulsion, that is, each particle was surrounded by the Halocarbon grease. Isolating individual particles with grease minimized the mass transfer of water vapor from unfrozen particles to frozen particles, and thus, the concentration of individual particles remained constant throughout the experiment. To check the effect of Halocarbon grease on the freezing properties of aqueous particles, we measured the homogeneous freezing temperatures of $(NH_4)_2SO_4-H_2O$ particles with and without the grease present. These results were in agreement, within experimental uncertainty, providing evidence that Halocarbon grease does not affect the freezing of our aqueous particles.

During the course of an experiment, the particles were observed with a microscope via two focusing eyepieces and a video camera (Sony XC 75) connected to a videotape recorder. We could easily observe phase transitions in the particles due to a change in light scattering. For example, each individual particle would suddenly turn dark on freezing. Furthermore, we could clearly distinguish between liquid particles, completely solid particles, and liquid particles with solid inclusions. Consequently, we were able to determine homogeneous nucleation temperatures, dissolution temperatures, and heterogeneous nucleation temperatures of individual particles.

2.2. Differential Scanning Calorimetry. We also used differential scanning calorimetry (DSC) to conduct heterogeneous freezing experiments on aqueous−oil emulsions. The experimental technique is described in detail elsewhere.[15,32] Briefly, emulsions were prepared by mixing 0.4 mL of an aqueous solution with 5.0 mL of an lanolin−Halocarbon oil solution and then shaking the resulting mixture with a high-speed mixer for approximately 5 min. A commercial Perkin-Elmer DSC-7 instrument was used for the calorimetric experiments. The DSC technique involved monitoring the differential energy required to keep both a sample (emulsion) and a reference (lanolin−Halocarbon oil mixture) at the same temperature, while the temperature was increased or decreased. The changes in the differential energy as a function of temperature were plotted as thermograms, and peaks in the thermograms indicated phase transitions. The aqueous particles in the emulsions had sizes ranging from 5 to 15 μm, as determined with the microscope.

2.3. Ammonium Sulfate Experiments. These experiments consisted of thermally cycling $(NH_4)_2SO_4-H_2O$ particles with

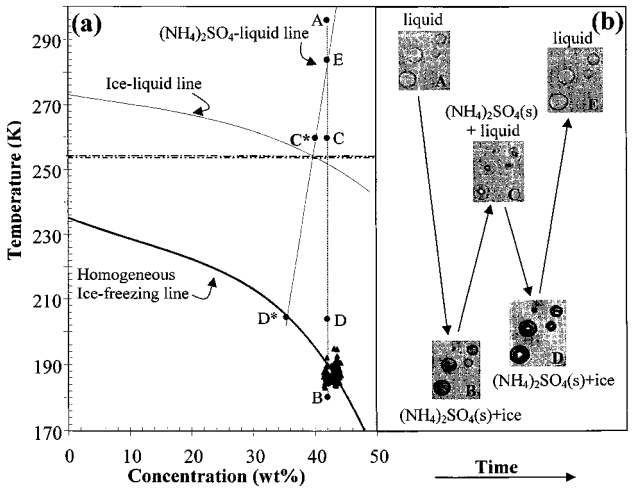

Figure 1. (a) Temperature vs concentration phase diagram for $(NH_4)_2SO_4-H_2O$.[30] The thin solid lines are the solid−liquid equilibrium curves for ice and $(NH_4)_2SO_4$ and the dash−dotted line represents the ice−$(NH_4)_2SO_4$ eutectic temperature. The thick solid line indicates the homogeneous ice-freezing data reported by Bertram et al.[17] for $(NH_4)_2SO_4-H_2O$ particles. The solid triangles represent the homogeneous freezing events in our experiments. The dotted line represents the thermal history of the particles. The points A−E along the dotted line indicate the different stages (see text for detail) in the thermal cycle. While points A, B, and E also indicate the liquid composition of the particles, points C* and D* indicate the concentration of the liquid in equilibrium with solid $(NH_4)_2SO_4$ at stage C and D of the experiment. (b) Photographs taken at various stages of the thermal cycle as a function of time.

concentrations between 41.3 and 44.6 wt % and determining the phase transition temperatures of the particles during the thermal cycling. The composition and temperature of the particles during these experiments are shown in Figure 1a, and photographs of the particles taken during each stage of the temperature-cycling experiments are shown in Figure 1b. The labels in the photographs in Figure 1b correspond to points A−E in Figure 1a. The vertical and horizontal positions of the photographs indicate the temperature and experimental time at which they were taken during the course of the experiment.

First, the particles were cooled from room temperature (point A in Figure 1a) to 183 K (point B in Figure 1a) at the rate of 10 K min^{-1}. This resulted in ice and solid ammonium sulfate nucleating in the particles. The particles were then heated to a temperature above the $(NH_4)_2SO_4-$ice eutectic temperature (254.2 K, dash−dotted line in Figure 1a), but below the $(NH_4)_2SO_4-$liquid equilibrium line (point C in Figure 1a). Note that the temperature that corresponds to point C varied from experiment to experiment, but in all cases it was above the eutectic temperature and below the $(NH_4)_2SO_4$ dissolution temperature. At point C, each particle consisted of an internal mixture of crystalline $(NH_4)_2SO_4$ in equilibrium with a liquid $(NH_4)_2SO_4-H_2O$ solution with composition C*. The presence of the solid core is clearly visible in Figure 1b, photograph C. The identity of the crystalline core, $(NH_4)_2SO_4$, was determined from the phase diagram. We will refer to the temperature at point C as the "conditioning temperature" throughout the remainder of this paper. After the particles were held at the conditioning temperature for approximately 5 min, the cell was slowly cooled at 1 K min^{-1} until heterogeneous freezing of ice on solid $(NH_4)_2SO_4$ was observed (point D in Figure 1a). In all experiments, this slow cooling rate was chosen to allow the liquid in the particles to maintain equilibrium with solid $(NH_4)_2SO_4$ such that the liquid assumes its equilibrium composition

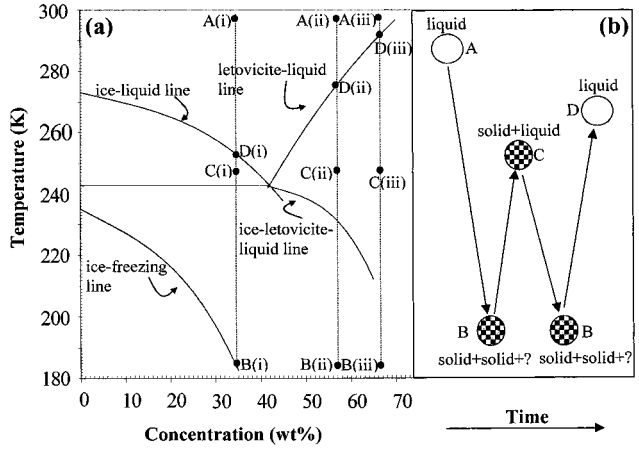

Figure 2. (a) Temperature vs concentration phase diagram for $NH_4HSO_4-H_2O$.[30] The ice-freezing line represents the homogeneous freezing data for ice in $NH_4HSO_4-H_2O$ reported by Koop et al.[15] The points A−D indicate the different stages in the thermal cycle (see text for detail) for particles with three different concentrations i−iii (Note: only the two-dimensional phase diagram for $NH_4HSO_4-H_2O$ is shown but, once letovicite crystallizes in solution, the solution becomes more acidic and leaves the two-dimensional space.) (b) Pictorial illustration of the phases we expected to detect in $NH_4HSO_4-H_2O$ particles at different stages of the thermal-cycling experiments.

D*. We have also performed heterogeneous freezing experiments at cooling rates of 3 and 5 K min^{-1}. The results obtained in these experiments agree with the results obtained at a cooling rate of 1 K min^{-1}, within experimental uncertainty. These results provide evidence that the solid is always in equilibrium with the liquid when the particles are cooled at 1 K min^{-1}. Finally, the temperature of the cell was increased at the rate of 1 K min^{-1} until the solid completely dissolved (point E in Figure 1a). From the dissolution temperatures, we calculated the compositions of the particles using a thermodynamic model.[30]

2.4. Ammonium Bisulfate Experiments. Temperature-cycling experiments were carried out on ammonium bisulfate particles with the following concentrations: 36 wt % (experiment i), 57 wt % (experiment ii), and 68 wt % (experiment iii). In each experiment, we thermally cycled the particles in a manner similar to that in the ammonium sulfate experiments described above. The three vertical lines in Figure 2a represent the temperature and composition during each experiment. The diagram in Figure 2b illustrates the expected morphology of the particles at each stage of the temperature-cycling experiments. First, the particles were cooled from room temperature (points A(i), A(ii), and A(iii) in Figure 2a) to 183 K (points B(i), B(ii), and B(iii) in Figure 2a) at 10 K min^{-1} and held at 183 K for approximately 30 min. This resulted in homogeneous freezing of the liquid particles. On the basis of the thermodynamic model by Clegg et al.,[30] it was possible for three solid phases to be present in the particle at 183 K, but we were unable to determine whether the third phase crystallized in the particles. The particles were then warmed at 1 K min^{-1} to a temperature below the solid−liquid coexistence line (points C(i), C(ii), and C(iii) in Figure 2a). At the conditioning temperatures (C(i), C(ii), and C(iii)) the particles contained both liquid and solid in equilibrium. After being held at points C(i), C(ii), and C(iii) for approximately 5 min, the particles were then slowly cooled at 1 K min^{-1} to 183 K (points B(i), B(ii), and B(iii) in Figure 2a) and then held at that temperature for approximately 60 min. Finally, the cell was warmed at 1 K min^{-1} to determine the concentrations from their equilibrium dissolution temperatures (points Di, Dii, and Diii in Figure 2a). From these thermal-cycling experiments, we determined both the homogeneous freezing temperatures and heterogeneous freezing temperatures of the individual particles.

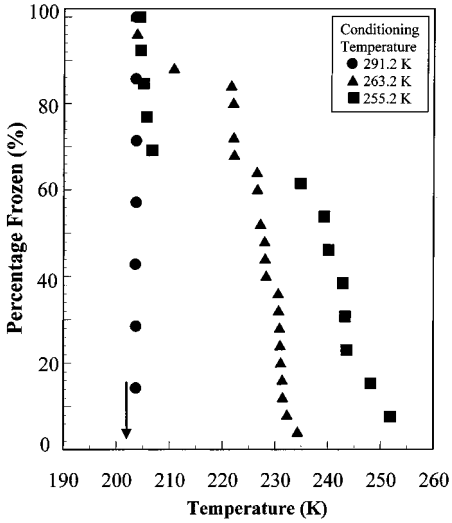

Figure 3. Percentage of drops frozen as a function of temperature for $(NH_4)_2SO_4-H_2O$ particles. The particles were cooled at 1 K min^{-1}. Solid circles are results from experiment with a conditioning temperature of 291.2 K, the solid triangles correspond to 263.2 K, and the solid squares correspond to a conditioning temperature of 255.2 K. The arrow indicates the expected homogeneous freezing temperature, 202.2 K, for homogeneous nucleation of a $(NH_4)_2SO_4-H_2O$ solution in equilibrium with a solid $(NH_4)_2SO_4$ core. This temperature was calculated as the point of intersection between the $(NH_4)_2SO_4$−liquid equilibrium line and the homogeneous ice-freezing line (see Figure 1a).

3. Results and Discussion

3.1. Ammonium Sulfate. The solid triangles in Figure 1a represent the homogeneous freezing temperatures determined with the microscope during several temperature-cycling experiments. These freezing temperatures, which are in excellent agreement with the homogeneous ice-freezing results reported by Bertram et al.[17] (thick solid line), did not vary from one experiment to the next, within the uncertainty of the measurements. In contrast, the heterogeneous ice-freezing temperatures varied as a function of the conditioning temperature (see Figure 1a) used in the thermal-cycling experiments. Shown in Figure 3 are heterogeneous freezing temperatures from three separate experiments. The conditioning temperatures used in each experiment are indicated in the figure. The higher the conditioning temperature the lower is the heterogeneous freezing temperature. We also determined heterogeneous freezing temperatures of aqueous $(NH_4)_2SO_4$−oil emulsions using differential scanning calorimetry. The emulsions were thermally cycled in the same manner as the microscope experiments. The temperatures at which the $(NH_4)_2SO_4-H_2O$ particles froze heterogeneously in these DSC experiments also depended on the conditioning temperature "C". Figure 4 shows the median heterogeneous freezing temperatures as a function of the conditioning temperature, determined from the microscope and DSC experiments. The DSC and microscope results display a similar trend: heterogeneous freezing occurs at warm temperatures if the conditioning temperature is close to, but warmer than, the eutectic temperature.

What could be the physical reasons for these observations? Figure 5a shows the morphology of the solid when a conditioning temperature of 291.2 K was used, and Figure 5b shows the morphology when a conditioning temperature of 255.2 K was

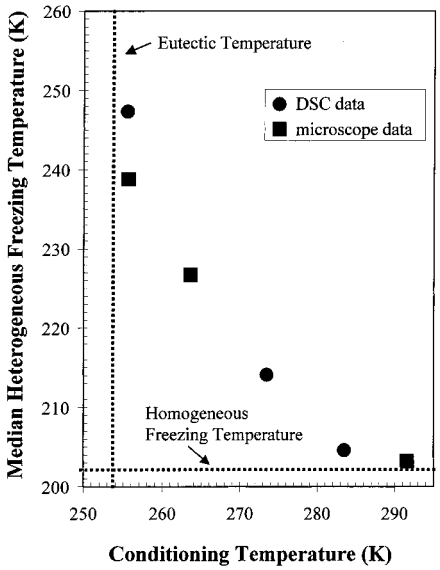

Figure 4. Plot of the median heterogeneous freezing temperatures as a function of the conditioning temperature "C", determined with the microscope and the DSC experiments. The DSC and microscope results illustrate that heterogeneous freezing of ice on ammonium sulfate occurred at warmer temperatures if the conditioning temperature was closer to the $(NH_4)_2SO_4-H_2O$ eutectic temperature.

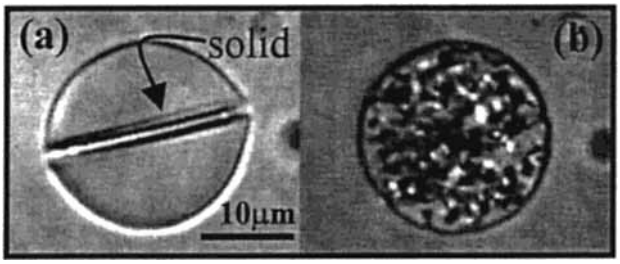

Figure 5. Photographs of a $(NH_4)_2SO_4-H_2O$ particle with a crystalline $(NH_4)_2SO_4$ core produced with conditioning temperatures of (a) 291.2 K and (b) 255.2 K. The photographs are of the same particle; since both photographs were taken at the same temperature (255.1 K), the mass of solid ammonium sulfate in the particle is the same in both cases.

used. The photographs are of the same particle and since both photographs were taken at the same temperature (at 255.1 K), the mass of solid ammonium sulfate in the particle was the same in both cases. These figures show that the surface area of the solid changes drastically with the conditioning temperature. We have performed several heterogeneous freezing experiments and the same trend was observed in all cases: If the conditioning temperature was close to the dissolution temperature, but not above the $(NH_4)_2SO_4-$liquid equilibrium line, the structure of the solid in equilibrium with aqueous particle resembled Figure 5a. But if the conditioning temperature was close to the eutectic temperature, the particle resembled Figure 5b. For the intermediate case, the size of the solid crystals was between the size of the microcrystals and the size of the large crystals. These observations indicate that the trend in Figure 4 is due to the surface area and surface microstructure of the solid ammonium sulfate.

Using DSC, we were also able to observe the solid−solid transition of ammonium sulfate, α and β forms, as reported by Martin[20,29] and Bajpai et al.[33] However, since the conditioning temperature was always warmer than the temperature for $\alpha-\beta$ ammonium sulfate solid−solid transition, we do not think the solid−solid phase transition affected heterogeneous freezing of the particles.

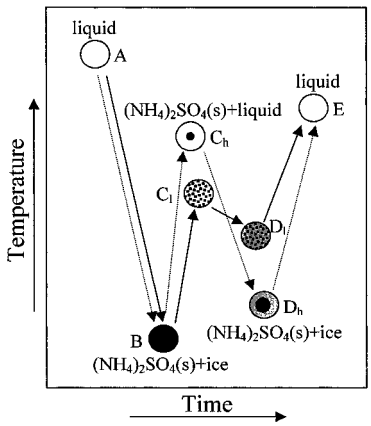

Figure 6. Schematic to explain the dependence of the surface area and morphology of solid $(NH_4)_2SO_4$ cores on the conditioning temperature in the thermal cycle. When the frozen particles (indicated by B) were warmed slightly above the eutectic, ice melted and left behind numerous microcrystals of $(NH_4)_2SO_4$ in each particle (C_l). When these particles were cooled without further warming, they readily froze because of the enhanced surface area available for nucleation (indicated by D_l). However, when the temperature of these particles was raised further, to C_h, the microcrystals began to melt and eventually only one or two microcrystals remained. Subsequent cooling of these particles resulted in only one or two large crystals in each particle, hence, minimizing the surface area of solid $(NH_4)_2SO_4$. These particles froze heterogeneously at D_h.

Figure 6 illustrates the surface area and surface microstructure changes we observe with the microscope during the temperature-cycling experiments and explains the relationship between the conditioning temperature and the morphology of the solid ammonium sulfate. In all experiments, the $(NH_4)_2SO_4-H_2O$ particles were first cooled from room temperature (point A in Figure 6) to 183 K (point B). Then the temperature was increased to slightly above the eutectic temperature. At this point, ice melted and left behind numerous microcrystals of ammonium sulfate in each particle. What happened next, after the microcrystals had been left behind, determined the surface area of the solid, and hence, the heterogeneous freezing temperature. If these $(NH_4)_2SO_4-H_2O$ particles were subsequently cooled (from a low conditioning temperature C_l in Figure 6) without further warming, they readily froze (at temperature D_l in Figure 6). However, if the temperature of these particles was raised further to a higher conditioning temperature, C_h, most of the microcrystals dissolved, leaving behind only one or two microcrystals. As these particles were cooled, the microcrystals grew in size, resulting in only one or two large crystals in each particle prior to heterogeneous nucleation. Since the surface area of the solid ammonium sulfate was minimized in this case, these particles supercooled to a lower temperature and froze heterogeneously at a temperature that corresponds to point D_h in Figure 6.

The above results show that the heterogeneous freezing temperature depends on the thermal history of the crystals. In addition, these results show that there is a clear trend between the surface area of the ammonium sulfate crystals and the heterogeneous freezing temperature. This is consistent with classical nucleation theory, which predicts that the heterogeneous freezing rate is proportional to the surface area.[4] From the microscope images we were able to determine the surface area of the large crystals; however, we were unable to determine the surface area of the microcrystals. Consequently, we could not ascertain if the change in heterogeneous nucleation temperature was due solely to a change in surface area. We have done calculations (based on classical nucleation theory) indicat-

ing that the required variation in surface area between large crystals and microcrystals would be beyond a physically reasonable quantity for surface area alone to be responsible for the variation in heterogeneous freezing temperatures. The difference in heterogeneous freezing temperatures shown in Figure 4 may also be due to the surface microstructure of the crystals (differences in surface defects of the crystals) since heterogeneous nucleation may occur predominately at surface defects such as cracks, steps, or dislocations. These surface defects may be enhanced on the microcrystals that are produced at fast crystal growth rates due to the high supersaturations at point B. In comparison, when the crystals were prepared by growing one or two microcrystals, the number of surface defects may be significantly reduced because the crystal growth rate is low, thus allowing for ion reorientation. Yet another possibility is that the heterogeneous freezing results may be due to preactivation, which is a well-known phenomenon in heterogeneous nucleation theory.[4,34] Initial formation of solid ammonium sulfate in the presence of ice may modify the crystalline structure of $(NH_4)_2SO_4$ at the interface. This modified surface may have sites that closely match the ice lattice (activated sites). If the temperature is increased only slightly above the eutectic temperatures, these activated sites may continue to exist on the solid ammonium sulfate surface, and as a result, heterogeneous freezing of ice may occur at much higher temperatures. On the other hand, the activated sites may not continue to exist if a conditioning temperature much warmer than the eutectic is used. Surface area, surface microstructure, and preactivation of surface sites, are all possible explanations for our heterogeneous freezing results. All these possibilities are dependent on the thermal history of the particles.

In the experiments where only one or two large solid ammonium sulfate crystals were present in each particle, the average solid surface in each individual particle was 380 ± 260 μm^2. The median heterogeneous freezing temperature of these particles was 203.7 K. The temperature required for homogeneous nucleation of the ammonium sulfate solution that was in equilibrium with the ammonium sulfate crystals was calculated using the model by Clegg et al.[30] and the homogeneous ice-freezing curve determined by Bertram et al.[17] (this corresponds to the intersection point of the $(NH_4)_2SO_4$−liquid line and the homogeneous ice-freezing line in Figure 1a). This freezing temperature, 202.2 K, is indicated in Figure 3 with an arrow. The calculated homogeneous ice-freezing temperature is only slightly lower than the median heterogeneous ice-freezing temperature of particles with one or two large $(NH_4)_2SO_4$ crystals, which indicates that a surface area of 380 ± 260 μm^2/particle does not significantly increase the rate of freezing of ammonium sulfate particles in our experiments.

We can use the experimental conditions to estimate an upper bound for the heterogeneous ice nucleation rate coefficient J_{het} on single $(NH_4)_2SO_4$ crystals. None of the 43 particles investigated crystallized at temperatures between 204 and 254.2 K. To estimate an upper limit for J_{het}, we take the minimum surface area of 120 μm^2 (=380−260 μm^2) and an observation time of 60 s at each 1 K temperature interval (the cooling rate was 1 K min^{-1}). Using Poisson statistics,[35] this yields an upper limit for $J_{het} \leq 1.5 \times 10^{-5}$ s^{-1} μm^{-2} with a confidence level of 99%.

Chen et al.[36] studied heterogeneous nucleation of ice by effloresced $(NH_4)_2SO_4$ particles. In these experiments the particles were completely crystalline until the deliquescence point was reached. In contrast, the particles in our experiments were always partially crystalline. Chen et al.[36] did not observe a decrease in the ice saturation ratio required for freezing in the effloresced $(NH_4)_2SO_4$ experiments when compared to ice formation in completely liquid $(NH_4)_2SO_4$ particles, indicating that crystalline $(NH_4)_2SO_4$ is a poor heterogeneous nuclei for ice. This result is consistent with the results we obtained when the solid was in the form of large crystals rather than microcrystals.

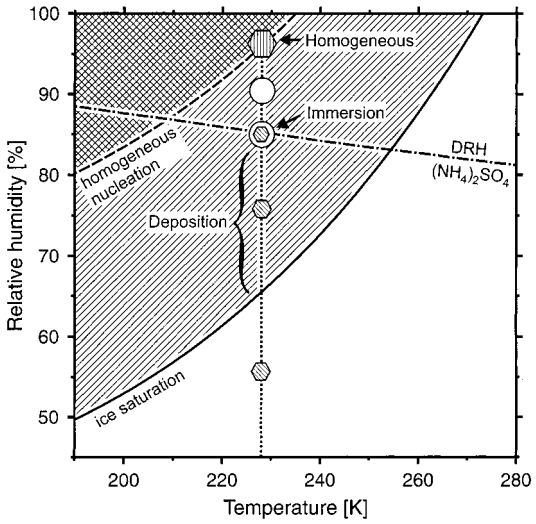

Figure 7. Hypothetical atmospheric trajectory of an initially dry $(NH_4)_2SO_4$ crystal (shown as the dotted line) in a temperature vs relative humidity phase diagram. The solid line is the ice saturation line and the dashed line represents the parametrization for homogeneous ice nucleation from liquid aqueous aerosols.[26] In the light shaded region ice is supersaturated whereas above the dashed curve (indicated as the dark shaded region) homogeneous ice nucleation will occur. The dash−dotted line indicates deliquescence relative humidity of $(NH_4)_2SO_4$ crystals as calculated using the model of Clegg et al.[30] For a detailed discussion, see text.

The trajectories in our experiments (temperature and concentration histories) are not common in the atmosphere. Nevertheless, there is a range of atmospheric conditions for which our results are applicable.

The first situation is when the ratio of ammonia-to-sulfate in the atmospheric aerosol is exactly 2:1. In these cases, at low relative humidities, the particles will be completely dry ammonium sulfate. When the temperature decreases and the relative humidity increases, the particles will deliquesce and temporarily exist as a solid−liquid mixture. This is schematically illustrated in Figure 7. The dotted line shows a hypothetical atmospheric trajectory of an initially dry $(NH_4)_2SO_4$ crystal (at low relative humidity) in a rising air parcel. Upon increasing relative humidity, ice becomes supersaturated above the solid line and, hence, the dry $(NH_4)_2SO_4$ crystal can serve as ice nuclei in the deposition mode. If ice deposition nucleation does not occur, the $(NH_4)_2SO_4$ crystal will start to deliquesce once the appropriate deliquescence relative humidity value (dash−dotted line) is reached. At this point the $(NH_4)_2SO_4$ crystal will dissolve and intermediately form a crystalline core within a $(NH_4)_2SO_4$ solution. During the time it takes the crystal to fully deliquesce, ice nucleation via the immersion freezing mode may occur. If not, the particle will fully deliquesce and ice nucleation will only occur when the homogeneous ice nucleation limit (dashed line) is reached.

Our results might also be applicable when the ammonia-to-sulfate ratio in atmospheric particles is nonstoichiometric. In these cases, the particles can exist as partially crystalline ammonium sulfate, i.e., internally mixed liquid−solid particles, over a wide range of conditions in the atmosphere. This is likely the dominant situation in the atmosphere since the conditions

required for forming perfectly stoichiometric particles are probably rare. For nonstoichiometric particles, the ammonium sulfate crystals will be in equilibrium with a nonstoichiometric solution. This is in contrast to our ammonium sulfate experiments where solid ammonium sulfate was always in equilibrium with a solution having a 2:1 ratio of ammonia-to-sulfate. Despite this fact, we suggest that the freezing temperatures of nonstoichiometric particles containing solid ammonium sulfate can be predicted on the basis of the ice saturations required for heterogeneous freezing determined in our experiments. For example, we propose on the basis of our freezing results that ice saturations only slightly larger than 1 are required to freeze nonstoichiometric particles containing microcrystals of ammonium sulfate. This assumes that the freezing temperatures can be predicted on the basis of ice saturations regardless of the stoichiometry of the solution, which has been shown to be applicable for homogeneous ice nucleation from aqueous solutions.[26]

We can estimate the fraction of $(NH_4)_2SO_4-H_2O$ particles (ammonia-to-sulfate ratio 2:1) in the atmosphere that will freeze heterogeneously during deliquescence using the J_{het} determined in our experiments. For this estimation we assume that during deliquescence each atmospheric particle consists of a 0.5 μm $(NH_4)_2SO_4$ crystal with a surface area of $\sim$0.8 μm^2 that is in equilibrium with the liquid (here we assume a spherical shape for the crystals, but similar results are obtained if we assume a cylindrical shape). On the basis of these assumptions, less than 10^{-4}% of these aerosol particles would be frozen after 10 s, less than 0.7% after 10 min, and less than 4.2% after 1 h at temperatures above 204 K. Since these estimates are based on upper limits for J_{het}, the frozen aerosol fraction is likely to be significantly smaller than the values calculated here. The deliquescence process of an initially dry $(NH_4)_2SO_4$ may take between a few seconds and several minutes in the atmospheric situation depending on the rate at which the relative humidity increases and also on the absolute water vapor pressure. As a result, at maximum only a small fraction of the aerosols will have nucleated ice during deliquescence. On the other hand, depending on whether microcrystals form upon efflorescence or not, the ice nucleation ability of $(NH_4)_2SO_4$ crystals might be significantly enhanced in the atmospheric situation. We conclude that it is important to understand the surface area and microstructure of atmospheric $(NH_4)_2SO_4$ crystals in order to evaluate their ability to act as heterogeneous ice nuclei.

3.2. Ammonium Bisulfate. The following concentrations were used in the ammonium bisulfate experiments: 36, 57, and 68 wt % NH_4HSO_4. In all cases, the ammonium bisulfate particles did not freeze homogeneously while cooling from room temperature to 183 K. The particles did freeze, however, at 183 K, but even at this temperature it took approximately 30 min for all the particles to freeze.

In the experiments with 36 wt % NH_4HSO_4 particles, the liquid was in equilibrium with ice after cooling to B and subsequently warming to the conditioning temperature C(i) (see Figure 2). When these particles were cooled to 183 K, heterogeneous freezing of a second solid phase was observed in less than 5% of the particles (see Table 1). An additional 26% of these particles froze when they were held at 183 K for approximately 60 min. The saturations with respect to sulfuric acid tetrahydrate (SAT), sulfuric acid hemihexahydrate (SAH), and letovicite in these liquid−solid particles at 183 K, calculated with a thermodynamic model,[30] are listed in Table 1. Since letovicite is highly supersaturated in these particles, the solid phase that nucleated on ice was probably letovicite. Even if a third solid phase crystallized in the particles, it would be below our detection limit. The saturations in Table 1, row 1, are lower limits to the saturations necessary for heterogeneous nucleation of a large fraction (>5%) of $NH_4HSO_4-H_2O$ particles with solid inclusions of ice at temperatures warmer than 183 K.

TABLE 1: Results from Heterogeneous Freezing Experiments on $NH_4HSO_4-H_2O$ Particles[a]

av concn	no. of particles	no. frozen above 183 K	no. frozen at 183 K	S_{ICE}^{183K}	S_{SAT}^{183K}	S_{SAH}^{183K}	S_{LET}^{183K}
i: 36 wt %	23	1	6	1.00	0.90	5.53	5252
ii: 57 wt %	12	2	5	1.57	0.12	0.87	1.00
iii: 68 wt %	10	0	2	1.04	2.22	40.84	1.00

[a] The experiments were conducted at three concentrations and the saturations with respect to the various solids at 183 K (S^{183K}_{SOLID}) were calculated using the thermodynamic model of Clegg et al., H_2O.[30] The 36 wt % particles contained solid inclusions of ice while the 57 and 68 wt % particles contained solid inclusions of letovicite. Less than 10% of the total particles exhibited heterogeneous freezing at temperatures warmer than 183 K.

In the experiments with 57 and 68 wt % NH_4HSO_4 particles, the liquid was in equilibrium with letovicite at the conditioning temperatures C(ii) and C(iii) in Figure 2. Only 9% of these particles froze heterogeneously above 183 K (see Table 1). An additional 38% froze when the particles were held at 183 K for approximately 60 min. The saturations with respect to ice, SAH, and SAT in these solid−liquid particles at 183 K are given in Table 1 (rows 2 and 3). In the 57 wt % particles, ice was the solid that nucleated heterogeneously, as it was the only solid supersaturated in the liquid. Ice, SAT, and SAH were all supersaturated in the 68 wt % experiments. On the basis of the results of Koop et al.,[15] we believe that SAT is the solid that nucleated heterogeneously on letovicite even though SAH has a higher supersaturation. We were unable to determine whether a third solid nucleated in these particles.

We also used DSC to investigate heterogeneous freezing of 57.7 wt % $NH_4HSO_4-H_2O$ particles. In these experiments, no heterogeneous freezing was detected above 183 K, which is consistent with the microscope results.

The solid in the $NH_4HSO_4-H_2O$ experiments was always in the form of large crystals rather than microcrystals. Producing microcrystals in these experiments proved to be difficult because most of the microcrystals were dissolved when the conditioning temperature was only 2 or 3 K above the eutectic. This can be explained by the slopes of the solid−liquid equilibrium curves for both ice and letovicite (see Figure 2). Because the solid−liquid equilibrium curves for both ice and letovicite are relatively flat, a slight increase in the conditioning temperature above the eutectic temperature results in significant dissolution of the crystalline solid (either ice or letovicite) in order to maintain the liquid−solid equilibrium. In contrast, the $(NH_4)_2SO_4$−liquid line is very steep, thus requiring only minor dissolution of $(NH_4)_2SO_4$ in order to maintain equilibrium.

Our heterogeneous freezing results show that when one or two large crystals of either ice or letovicite are present in $NH_4HSO_4-H_2O$ particles, the freezing temperature does not deviate significantly from the homogeneous freezing temperature of $NH_4HSO_4-H_2O$ particles. This is consistent with the $(NH_4)_2SO_4-H_2O$-freezing results. To find out whether microcrystals of letovicite or ice induce freezing at higher temperatures, as is the case with microcrystals of $(NH_4)_2SO_4$, will require additional experiments.

4. Summary and Conclusions

The heterogeneous freezing of $(NH_4)_2SO_4-H_2O$ and $NH_4HSO_4-H_2O$ particles by solid inclusions of crystallized $(NH_4)_2$-

SO_4, ice, and letovicite was investigated with optical microscopy and differential scanning calorimetry. The temperature at which ice nucleates heterogeneously from solution on solid $(NH_4)_2SO_4$ crystals was found to be dependent on the surface area and microstructure of the solid, as well as the thermal history of the particles. If the solid was in the form of microcrystals, the heterogeneous ice-freezing temperature was close to the eutectic temperature, but if the solid was in the form of large crystals, the freezing temperature was close to the homogeneous ice-freezing temperature. A surface area of 380 ± 260 μm^2/particle (large crystals only) did not significantly increase the rate of freezing of ammonium sulfate particles in our experiments. Although the estimated upper limit for the heterogeneous nucleation rate of ice (immersion mode), based on our experiments, does not rule out that single $(NH_4)_2SO_4$ crystals may act as heterogeneous ice nuclei in the atmosphere, we consider this to be unlikely. However, if atmospheric aerosols contain solid $(NH_4)_2SO_4$ in the form of microcrystals, with the associated surface defects and higher surface area, they might function as efficient heterogeneous ice nuclei.

In the case of $NH_4HSO_4-H_2O$ particles, where one or two large crystals of ice or letovicite were in equilibrium with a liquid, the heterogeneous freezing temperatures were close to the homogeneous freezing temperatures, similar to the $(NH_4)_2SO_4-H_2O$ experiments. This suggests that heterogeneous nucleation by ice or letovicite with a similar morphology is not an important atmospheric process.

This work shows that the morphology of crystalline solids can significantly change the heterogeneous freezing temperature and that heterogeneous nucleation of ice induced by crystalline salts (immersion mode) may be very important in the formation of UT clouds. We suggest further laboratory and field work to investigate the morphology of crystallized cores in atmospheric aqueous particles, as well as to determine the ice nucleation conditions and heterogeneous nucleation rates relevant for the formation of UT clouds.

Acknowledgment. This research was supported by grants from NASA's Upper Atmospheric Research Program and the National Science Foundation. We thank Chris Cassa for technical assistance. We also thank Scot Martin for helpful suggestions to improve the manuscript.

References and Notes

(1) Fu, Q.; Liou, K. N. *J. Atmos. Sci.* **1993**, *50*, 2008−2025.
(2) IPCC *The Science of Climate Change*; Cambridge University Press: New York, 1996.
(3) Liou, K. N. *Monthly Weather Rev.* **1986**, *114*, 1167−1199.
(4) Pruppacher, H. R.; Klett, J. D. *Microphysics of Clouds and Precipitation*; Kluwer Academic Publishers: Boston, 1997.
(5) Borrmann, S.; Solomon, S.; Avallone, L.; Toohey, D.; Baumgardner, D. *Geophys. Res. Lett.* **1997**, *24*, 2011−2014.
(6) Jaegle, L.; Jacob, D. J.; Brune, W. H.; Faloona, I.; Tan, D.; Heikes, B. G.; Kondo, Y.; Sachse, G. W.; Anderson, B.; Gregory, G. L.; Singh, H. B.; Pueschel, R.; Ferry, G.; Blake, D. R.; Shetter, R. E. *J. Geophys. Res.* **2000**, *105*, 3877−3892.
(7) Solomon, S.; Borrmann, S.; Garcia, R. R.; Portmann, R.; Thomason, L.; Poole, L. R.; Winker, D.; McCormick, M. P. *J. Geophys. Res.* **1997**, *102*, 21411−21429.
(8) Kley, D.; Crutzen, P. J.; Smit, H. G. J.; Vomel, H.; Oltmans, S. J.; Grassl, H.; Ramanathan, V. *Science* **1996**, *274*, 230−233.
(9) Jensen, E. J.; Toon, O. B.; Westphal, D. L.; Kinne, S.; Heysmfield, A. J. *J. Geophys. Res.* **1994**, *99*, 10421−10442.
(10) DeMott, P. J.; Rogers, D. C.; Kreidenweis, S. M. *J. Geophys. Res.* **1997**, *102*, 19575−19584.
(11) Vali, G. *J. Atmos. Sci.* **1994**, *51*, 1843−1856.
(12) Sassen, K.; Dodd, G. C. *J. Atmos. Sci.* **1988**, *45*, 1357−1369.
(13) Sassen, K.; Dodd, G. C. *J. Atmos. Sci.* **1989**, *46*, 3005−3014.
(14) Koop, T.; Ng, H. P.; Molina, L. T.; Molina, M. J. *J. Phys. Chem. A* **1998**, *102*, 8924−8931.
(15) Koop, T.; Bertram, A. K.; Molina, L. T.; Molina, M. J. *J. Phys. Chem. A* **1999**, *103*, 9042−9048.
(16) Bertram, A. K.; Patterson, D. D.; Sloan, J. J. *J. Phys. Chem.* **1996**, *100*, 2376−2383.
(17) Bertram, A. K.; Koop, T.; Molina, L. T.; Molina, M. J. *J. Phys. Chem. A* **2000**, *104*, 584−588.
(18) Cziczo, D. J.; Abbatt, J. P. D. *J. Geophys. Res.* **1999**, *104*, 13781−13790.
(19) Clapp, M. L.; Niedziela, R. F.; Richwine, L. J.; Dransfield, T.; Miller, R. E.; Worsnop, D. R. *J. Geophys. Res.* **1997**, *102*, 8899−8907.
(20) Martin, S. *Chem. Rev.* **2000**, *100*, 3403−3453.
(21) Talbot, R. W.; Dibb, J. E.; Loomis, M. B. *Geophys. Res. Lett.* **1998**, *25*, 1367−1370.
(22) Adams, P. J.; Seinfeld, J. H.; Koch, D. M. *J. Geophys. Res.* **1999**, *104*, 13791−13823.
(23) Dibb, J. E.; Talbot, R. W.; Scheuer, E. M.; Blake, D. R.; Blake, N. J.; Gregory, G. L.; Sachse, G. W.; Thornton, D. C. *J. Geophys. Res.* **1999**, *104*, 5785−5800.
(24) Heymsfield, A. J.; Milosevich, L. M.; Twohy, C.; Sachse, G.; Oltmans, S. *Geophys. Res. Lett.* **1998**, *25*, 1343−1346.
(25) Jensen, E. J.; Toon, O. B.; Tabazadeh, A.; Sachse, G. W.; Anderson, B. E.; Chan, K. R.; Twohy, C. W.; Gandrud, B.; Aulenbach, S. M.; Heymsfield, A.; Hallett, J.; Gary, B. *Geophys. Res. Lett.* **1998**, *25*, 1363−1366.
(26) Koop, T.; Luo, B. P.; Tsias, A.; Peter, T. *Nature* **2000**, *406*, 611−614.
(27) Heymsfield, A. J.; Miloshevich, L. M. *J. Atmos. Sci.* **1995**, *52*, 4302−4326.
(28) Tabazadeh, A.; Toon, O. B. *Geophys. Res. Lett.* **1998**, *25*, 1379−1382.
(29) Martin, S. T. *Geophys. Res. Lett.* **1998**, *25*, 1657−1660.
(30) Clegg, S. L.; Brimblecombe, P.; Wexler, A. S. *J. Phys. Chem. A* **1998**, *102*, 2137−2154.
(31) Imre, D. G.; Xu, J.; Tang, I. N.; McGraw, R. *J. Phys. Chem. A* **1997**, *101*, 4191−4195.
(32) Chang, H. Y. A.; Koop, T.; Molina, L. T.; Molina, M. J. *J. Phys. Chem. A* **1999**, *103*, 2673−2679.
(33) Bajpai, P. K.; Jain, Y. S.; Bist, H. D. *J. Raman Spectrosc.* **1990**, *21*, 327−332.
(34) Zhang, R. Y.; Leu, M. T.; Molina, M. J. *Geophys. Res. Lett.* **1996**, *23*, 1669−1672.
(35) Koop, T.; Luo, B. P.; Biermann, U. M.; Crutzen, P. J.; Peter, T. *J. Phys. Chem. A* **1997**, *101*, 1117−1133.
(36) Chen, Y. L.; DeMott, P. J.; Kreidenweis, S. M.; Rogers, D. C.; Sherman, D. E. *J. Atmos. Sci.* **2000**, *57*, 3752−3766.